A transverse isotropic model for microporous solids - Application to coal matrix adsorption and swelling

Nicolas Espinoza, Matthieu Vandamme, Patrick Dangla, Jean-Michel Pereira, S. Vidal-Gilbert

A transverse isotropic model for microporous solids - Application to coal matrix adsorption and swelling

D.N. Espinoza,[1] M. Vandamme,[1] P. Dangla,[1] J.-M. Pereira[1], and S. Vidal-Gilbert[2]

Corresponding author: D. N. Espinoza, Université Paris-Est, Laboratoire Navier (UMR 8205), ENPC, CNRS, IFSTTAR, 6-8 Av. Blaise Pascal, 77420, Champs-sur-Marne, FRANCE (nicolas.espinoza@enpc.fr)

[1]Université Paris-Est, Laboratoire Navier (UMR 8205), ENPC, CNRS, IFSTTAR, France

[2]Total S.A., Unconventional Gas Resources, France

Abstract. Understanding the adsorption-induced swelling in coal is critical for predictable and enhanced coal bed methane production. The coal matrix is a natural anisotropic disordered microporous solid. We develop an elastic transverse isotropic poromechanical model for microporous solids which couples adsorption and strain through adsorption stress functions, and expresses the adsorption isotherm as a multivariate function depending on fluid pressure and solid strains. Experimental data from the literature help inverting the anisotropic adsorptive-mechanical properties of Brzeszcze coal samples exposed to CO_2. Main findings include: (1) adsorption-induced swelling can be modeled by including fluid-specific and pressure-dependent adsorption stress functions into equilibrium equations, (2) modeling results suggest that swelling anisotropy is mostly caused by anisotropy of the solid mechanical properties, and (3) the total amount of adsorbed gas measured by immersing coal in the adsorbate overestimates adsorption amount compared to in-situ conditions up to $\sim$20%. The developed fully coupled model can be upscaled to determine the coal seam permeability through permeability-stress relationships.

1. Introduction

The understanding of adsorption of gases in mesoporous and microporous solids is important for applications in gas capture, gas separation, and gas desorption/adsorption in sedimentary rocks. Micropores are defined by the IUPAC as pores with width not exceeding 2 nm. We consider here a broader definition of microporous solids including porous solids with pores sized in the order of a few nanometers. Natural microporous solids include coal, kerogen, zeolites, and gas hydrates; while artificial microporous solids include microcarbon and metal organic frameworks among others [*Ravikovitch and Neimark*, 2006; *Mazumder et al.*, 2006; *Vandenbroucke and Largeau*, 2007; *Sloan and Koh*, 2008; *Kowalczyk et al.*, 2008; *Neimark et al.*, 2011]. From another point of view, microporous solids can be classified as regards their structure in crystalline (ordered structure: metal organic frameworks, zeolites, hydrates) or disordered (coal, kerogen, microporous carbon). Nano-sized micropores can host just a few fluid molecules. The adsorption of fluids in these pores can lead to their expansion or contraction depending on the pore size, geometry, and fluid-solid interaction [*Kowalczyk et al.*, 2008; *Pijaudier-Cabot et al.*, 2011; *Brochard et al.*, 2012]. Macroscopically, adsorption-driven changes of pore size or pressure upscale as strains (or stresses if strains are prescribed).

This coupling between strain and adsorption is particularly important in the context of underground adsorptive geomaterials, such as coal and organic shales [*Busch et al.*, 2008; *Weniger et al.*, 2010]. Hydrocarbon production from these reservoirs imposes significant changes in stresses coupled with adsorption or desorption leading to strains which affect the aperture and permeability of natural and generated fractures. The adsorption-strain

coupling is critical to defining production rates of natural gas from highly-adsorptive coal bed seams [*Palmer and Mansoori*, 1998; *Pan and Connell*, 2012].

The adsorption and swelling of various gases including carbon dioxide CO_2, methane CH_4, and nitrogen N_2 in coal has been largely studied in the past decades [*Reucroft and Sethuraman*, 1987; *Ceglarska-Stefanska and Czaplinski*, 1993; *Levine*, 1996; *Ceglarska-Stefanska and Zarebska*, 2002; *Mazumder et al.*, 2006; *Pini et al.*, 2009]. Adsorbed amounts are usually measured in the laboratory in terms of excess adsorbed amount, that is, the amount of fluid in excess of the amount of fluid which would occupy the pore volume in bulk conditions. In general for low-medium gas pressure, up to $\sim$10 MPa, the rule "the greater the pressure, the greater the total adsorbed amount" is valid. In this range, coal swelling is usually proportional to the amount of adsorbed gas. For higher pressures, the bulk fluid pressure compresses the solid skeleton and may prevail over adsorption-induced swelling [*Moffat and Weale*, 1954; *Pan and Connell*, 2007; *Hol and Spiers*, 2012]. In fact, recent studies show that the application of compressive confining stresses (and ensuing strains) to coal swollen and equilibrated with CO_2 at a certain pressure induce the expulsion of adsorbed gas [*Hol et al.*, 2011, 2012]. This desorption induced by mechanical stresses is not due to the loss of pore accessibility caused by permeability reduction upon the application of compressive external stresses, phenomenon which is also observed in coal [*Pone et al.*, 2009; *Wang et al.*, 2011].

Such a particular behavior of coal motivated the extension of the theory of poromechanics to include adsorption phenomena in microporous solids. *Brochard et al.* [2012] proposed a set of poromechanical equations valid for linear elastic isotropic microporous solids which considers as main variable the total amount of adsorbed fluid as a function

of fluid pressure and solid strain, without a need for introducing the notion of pore volume. The model is based on first principles, shows good swelling prediction capability, and eventually leads to the classical theory of poromechanics if adsorption is negligible.

Although *Brochard et al.* [2012] developed a model applicable to isotropic coal matrix, most sedimentary geomaterials are not isotropic. Vertical deposition and overburden at zero-lateral strain favor transverse isotropic symmetry [*Thomsen*, 1986; *Johnston and Christensen*, 1995; *Vernik and Nur*, 1992]. Anisotropic poromechanical responses can be quantified by the Biot effective stress coefficient tensor or equivalently by the Skempton tensor [*Cheng*, 1997; *Cowin*, 2004]. The mechanical and swelling properties of coal are notably anisotropic, with a major influence of the orientation respect to the bedding plane and the proximity to cleats [*Cody et al.*, 1988; *Levine*, 1996; *Hol and Spiers*, 2012; *Day et al.*, 2010; *Morcote et al.*, 2010].

This article presents an extension of the poromechanical model for adsorptive microporous solids developed by *Brochard et al.* [2012] to take into account material properties anisotropy. The anisotropy is integrated for both adsorption-induced phenomena and mechanical properties, and it is implemented by means of a transverse isotropic model pertinent to sedimentary rocks. The model is used to invert the anisotropic adsorptive-mechanical properties of a sample of Brzeszcze coal tested by *Hol and Spiers* [2012]. The model offers further insight into the relationship between swelling and adsorption.

2. Model formulation

The model is based on energy conservation and follows from a thermodynamical formulation. A more detailed formulation developed for isotropic microporous solids is available elsewhere [*Brochard et al.*, 2012]. We aim at developing the poromechanical equations for

adsorbing microporous solids which exhibit transverse isotropic properties. The interested reader will find similar theoretical developments applied to various poromechanical problems in [*Coussy*, 2004, 2010]. The theory of poroelasticity for anisotropic macroporous solids has been revisited by several authors [*Cheng*, 1997; *Coussy*, 2004; *Cowin*, 2004].

2.1. Energy conservation

Consider a representative elementary volume of a microporous solid with free energy per unit volume f [J/L], subjected to stresses σ_{ij} [Pa], and whose adsorbed fluid has a molar chemical potential μ [J/mol]. Energy conservation under isothermal conditions dictates

$$df = \sum_{i,j} \sigma_{ij} d\varepsilon_{ij} + \mu dn \tag{1}$$

being ε_{ij} the strain tensor [-], and n the number of moles of fluid per unit volume of undeformed microporous solid [mol/L]. Strains are calculated respect to the original configuration (Lagrangian formulation). By changing variables, the following holds

$$d(f - n\mu) = \sum_{i,j} \sigma_{ij} d\varepsilon_{ij} - n d\mu \tag{2}$$

The first term to the right of the equality represents the incremental work done by stresses and the second represents the change of energy associated to changes in the chemical potential of the fluid phase. The development of the model consists in finding expressions to the variables σ_{ij}, and n as a function of the other variables. Volume average considerations, Maxwell's relations, and the Gibbs-Duhem equation are used to this purpose.

2.2. Derivation of equations of state

Let us apply Maxwell's relation on the previous energy conservation equality (Eq. 2),

$$\frac{\partial^2(f-n\mu)}{\partial\varepsilon_{ij}\partial\mu} = \frac{\partial^2(f-n\mu)}{\partial\mu\partial\varepsilon_{ij}} \tag{3}$$

Derivation leads to

$$\left.\frac{\partial\sigma_{ij}}{\partial\mu}\right|_{\varepsilon_{kl\neq ij}} = -\left.\frac{\partial n}{\partial\varepsilon_{ij}}\right|_{\mu,\varepsilon_{kl\neq ij}} \tag{4}$$

The equality holds for strains $\varepsilon_{kl\neq ij}$ constant. By integrating this equation on the molar chemical potential μ we obtain the following equation

$$\sigma_{ij} = \Psi_{ij}(\underline{\underline{\varepsilon}}) - \int_{-\infty}^{\mu}\left.\frac{\partial n}{\partial\varepsilon_{ij}}\right|_{\mu,\varepsilon_{kl\neq ij}} d\mu \tag{5}$$

where Ψ_{ij} results from this integration and, thus, is a function independent from the fluid chemical potential μ. The molar chemical potential μ can be re-written using Gibbs-Duhem relation for isothermal conditions $d\mu = \overline{V}_b(p)dp$, where $\overline{V}_b$ is the molar volume of the fluid in bulk conditions [L/mol] as a function of temperature and pressure, and p is the thermodynamic pressure of the fluid [Pa] defined as the pressure of the bulk fluid at the same chemical potential as the adsorbed phase. Hence, Eq. (5) can be written as follows

$$\sigma_{ij} = \Psi_{ij}(\underline{\underline{\varepsilon}}) - \int_{0}^{p}\left.\frac{\partial n}{\partial\varepsilon_{ij}}\right|_{p,\varepsilon_{kl\neq ij}} \overline{V}_b(p)dp \tag{6}$$

The first term to the right of the equality Ψ_{ij} represents the "dry" response of the specimen to strains (without the fluid phase) and the integral term represents the response

to fluid loading as a function of fluid pressure and solid strain. For example, assuming linear elasticity, isotropic material properties, and that the fluid is in bulk conditions, *Brochard et al.* [2012] show that Eq. (6) permits recovering the classical equations of poroelasticity $\sigma = K\epsilon - bp$, where K is the drained bulk modulus, ϵ is the volumetric strain, and b is the Biot coefficient).

2.3. Simplification for transverse isotropic coal

Linear elastic transverse isotropy. The functions Ψ_{ij} depend on strains $\underline{\underline{\varepsilon}}$ only, hence, any linear or non-linear elastic constitutive law may be used. We use transverse isotropic linear elasticity for functions Ψ_{ij} in this formulation. Transverse isotropic materials are defined by an axis of symmetry in their elastic properties (say axis 3 in this development). The reduced stiffness matrix in Voigt notation C_{ij} has 5 independent constants. Thus, the "dry" response of a generic transversely isotropic porous solid $\sigma_{ij} = \Psi_{ij}(\underline{\underline{\varepsilon}})$ is

$$\begin{cases} \sigma_{11} &= C_{11}\varepsilon_{11} + C_{12}\varepsilon_{22} + C_{13}\varepsilon_{33} \\ \sigma_{22} &= C_{12}\varepsilon_{11} + C_{11}\varepsilon_{22} + C_{13}\varepsilon_{33} \\ \sigma_{33} &= C_{13}\varepsilon_{11} + C_{13}\varepsilon_{22} + C_{33}\varepsilon_{33} \\ \sigma_{23} &= 2C_{44}\varepsilon_{23} \\ \sigma_{31} &= 2C_{44}\varepsilon_{31} \\ \sigma_{12} &= (C_{11} - C_{12})\varepsilon_{12} \end{cases} \tag{7}$$

Deformation can be expressed in terms of engineering elastic constants E (Young modulus in direction 1 and 2), E_3 (Young modulus in direction 3), ν (Poisson ratio in plane 1-2), ν_3 (Poisson ratio in planes 1-3 and 2-3), and G_3 (shear modulus in plane 1-3 and 2-3) as $\varepsilon_{kl} = \Psi'_{kl}(\underline{\underline{\sigma}})$,

$$\begin{cases} \varepsilon_{11} &= (1/E)\sigma_{11} - (\nu/E)\sigma_{22} - (\nu_3/E_3)\sigma_{33} \\ \varepsilon_{22} &= -(\nu/E)\sigma_{11} + (1/E)\sigma_{22} - (\nu_3/E_3)\sigma_{33} \\ \varepsilon_{33} &= -(\nu_3/E_3)\sigma_{11} - (\nu_3/E_3)\sigma_{22} + (1/E_3)\sigma_{33} \\ 2\varepsilon_{23} &= (1/G_3)\sigma_{23} \\ 2\varepsilon_{31} &= (1/G_3)\sigma_{31} \\ 2\varepsilon_{12} &= [2(1+\nu)/E]\sigma_{12} \end{cases} \tag{8}$$

Multivariate adsorption isotherm. The derivative $\partial n/\partial \varepsilon_{ij}|_{p,\varepsilon_{kl\neq ij}}$ in the right hand side of Eq. (6) can be further developed if the total amount of adsorbed fluid $n(p, \varepsilon_{ij})$ is known as a function of the thermodynamic pressure of the fluid p and the strains of the microporous solid ε_{ij}. Considering small strains, this multivariate adsorption isotherm can be expressed as a first-order expansion with respect to strains, such that,

$$n(p, \varepsilon_{ij}) = n_0(p)[1 + c_1(p)\varepsilon_{11} + c_2(p)\varepsilon_{22} + c_3(p)\varepsilon_{33}] \tag{9}$$

where $n_0(p) = n(p, \underline{\underline{0}})$ is the total amount of adsorbed fluid at zero solid strain, and $c_1(p)$, $c_2(p)$, $c_3(p)$ are the adsorption-strain coupling functions for each direction [-]. Coefficients $c_i(p)$ capture the coupling between adsorption and strain, and depend on fluid pressure, type of gas, pore shape and size distribution. *Brochard et al.* [2012] performed molecular simulations of CH_4 adsorption in disordered organic microporous solids and validated this first-order expansion (Eq. 9) in the isotropic case, for volumetric strains up to $\sim$10%. Such strains are sufficiently large to consider that this first-order expansion is valid for coal in practical conditions. We will consider that this validity remains in the case of transverse isotropy. Also, *Brochard et al.* [2012] show that adsorption-strain coupling coefficients can be negative when adsorption induces pore shrinkage or positive if pore expansion prevails. Transverse isotropy in the adsorption-strain coupling imposes $c_1(p) = c_2(p)$.

Various adsorbing materials, including coal exposed at moderate gas pressure, are well described by Langmuir adsorption isotherms as a function of pressure or more appropriately as a function of the fluid fugacity [*Fowler*, 1935; *Vandamme et. al.*, 2010; *Hol et al.*, 2011]. Hence, assuming a Langmuir-type of adsorption as a function of pressure for the undeformed microporous coal leads to

$$n_0(p) = n_0^{max} \frac{p}{\beta + p} \tag{10}$$

with n_0^{max} being the maximum total amount of adsorbed fluid at zero solid strain [mol/L], and β the Langmuir pressure [Pa] at which one half of the adsorption capacity is reached while keeping zero solid strain.

From Eq. (9) and (10), the derivatives of $n(p, \varepsilon_{ij})$ with respect to strains ε_{ij} result:

$$\left.\frac{\partial n}{\partial \varepsilon_{ij}}\right|_{p,\varepsilon_{kl\neq ij}} = c_i(p) n_0(p) \delta_{ij} \tag{11}$$

Eq. (9) implicitly assumes that the principal directions of the tensor $\partial n/\partial \varepsilon_{ij}|_{p,\varepsilon_{kl\neq ij}}$ coincide with the geometrical axes of symmetry. Hence, these derivatives are non-zero only with respect to strain components ε_{ii} and vanish for shear strains components ε_{ij} with $i \neq j$. Back to Eq. (6), adsorption-induced strains and stresses on the anisotropic microporous solid can be quantified with terms named $s_i^a(p) = \int_0^p \partial n/\partial \varepsilon_{ij}|_{p,\varepsilon_{kl\neq ij}} \overline{V}_b dp$, which, with the help of Eq. (11), become

$$s_i^a(p) = \int_0^p c_i(p) n_0(p) \overline{V}_b(p) dp \tag{12}$$

We call these terms "adsorption stresses" as motivated by an analogy with the theory formulated by *Ravikovitch and Neimark* [2006]. Physically, these terms quantify the stresses needed to keep the microporous solid at zero volumetric strain during adsorption.

Final equations. Combining the linear elastic constitutive equations (Eq. 7) with adsorption stresses (Eq. 12), the set of equations (Eq. 6) becomes

$$\begin{cases} \sigma_{11} = C_{11}\varepsilon_{11} + C_{12}\varepsilon_{22} + C_{13}\varepsilon_{33} - s_1^a(p) \\ \sigma_{22} = C_{12}\varepsilon_{11} + C_{11}\varepsilon_{22} + C_{13}\varepsilon_{33} - s_1^a(p) \\ \sigma_{33} = C_{13}\varepsilon_{11} + C_{13}\varepsilon_{22} + C_{33}\varepsilon_{33} - s_3^a(p) \\ \sigma_{23} = 2C_{44}\varepsilon_{23} \\ \sigma_{31} = 2C_{44}\varepsilon_{31} \\ \sigma_{12} = (C_{11} - C_{12})\varepsilon_{12} \end{cases} \tag{13}$$

The model relies on five mechanical parameters C_{11}, C_{33}, C_{12}, C_{13}, C_{44} (stiffness coefficients which can be expressed as a function of E, ν, E_3, ν_3, G_3), one fluid equation of state $\overline{V}_b(p)$ at a given temperature, two characteristic total adsorption parameters n_0^{max} and β for the microporous solid at zero strain, and two adsorption-strain coupling pressure-dependent functions $c_1(p)$ and $c_3(p)$.

3. Application example - Unconstrained coal swelling

Let us consider a piece of coal matrix immersed in CO_2 under unconstrained displacement boundary conditions (unjacketed: no membrane or wall, the solid is free to swell), such that CO_2 pressure applies isotropic loading and no shear on the solid ($\sigma_{11} = \sigma_{22} = \sigma_{33} = -p$; $\sigma_{ij} = 0$ for $i \neq j$). The coal is in thermodynamical equilibrium, thus, the chemical potential of the bulk fluid at pressure p is the same as the chemical potential of the adsorbed fluid. Isotropic loading in a transverse isotropic medium imposes $\varepsilon_{11} = \varepsilon_{22}$ in the general case $C_{11} \neq C_{12}$ (from Eq. 13), $\varepsilon_{11} = \varepsilon_{22} = \varepsilon_1$ the principal strain

on the bedding plane, and $\varepsilon_{33} = \varepsilon_3$ the principal strain perpendicular to the bedding plane, hence, Eq. (13) reduces to

$$\begin{cases} \sigma_{11} = \sigma_{22} \;=\; -p \;=\; (C_{11} + C_{12})\varepsilon_1 + C_{13}\varepsilon_3 - s_1^a(p) \\ \qquad \sigma_{33} \;=\; -p \;=\; 2C_{13}\varepsilon_1 + C_{33}\varepsilon_3 - s_3^a(p) \end{cases} \tag{14}$$

Let us write the principal strains ε_1 and ε_3 as function of stresses using the engineering elastic constants. Swelling strains result

$$\begin{bmatrix} \varepsilon_1 \\ \varepsilon_3 \end{bmatrix} = \begin{bmatrix} \frac{1-\nu}{E} & -\frac{\nu_3}{E_3} \\ -2\frac{\nu_3}{E_3} & \frac{1}{E_3} \end{bmatrix} \begin{bmatrix} s_1^a(p) - p \\ s_3^a(p) - p \end{bmatrix} \tag{15}$$

Recent experimental results show the swelling of cylindrical Brzeszcze coal specimens immersed in CO_2 up to 100 MPa of fluid pressure (specimen size 4mm length and 4mm diameter [*Hol and Spiers*, 2012]). Strains are measured in two perpendicular directions in the bedding plane (noted ε_x and ε_y), at 45° between the x and y axes, and perpendicular to the bedding plane (this latter noted ε_z). Results show a clear orthotropic swelling of coal specimens, being the strain perpendicular to the bedding plane the highest $\varepsilon_z > \varepsilon_y \sim \varepsilon_x$. We consider the major principal strain $\varepsilon_3 = \varepsilon_z$. We calculate the other two principal strains from the original data set based on the three strains measured in the bedding plane. Figures 1-a and 1-d show the principal strains for two coal specimens 364-1 and 364-2, as named in the source reference. Although the experimental results show an orthotropic response, we fit a transverse isotropic model in views of upscaling to coal seams with transverse isotropic properties and to reduce the number of inverted parameters. The experimental principal strain ε_3 and the mean of the experimental principal strains on the bedding plane $(\varepsilon_1 + \varepsilon_2)/2$ are used to validate the transverse isotropic model.

Additional data help us invert the coal adsorptive-mechanical properties; these data include: (1) total amount of adsorption in Brzeszcze coal immersed in CO_2 up to 15 MPa (estimated from excess adsorbed amount measurements at 45°C by *Gensterblum et al.* [2010] with best fitting adsorbed phase volume per unit mass of coal $V_{ads}/m_{coal} = 0.055$ cm^3/g - see Auxiliary Material); (2) the dry coal mass density $\rho \sim 1343$ kg/m^3 [*Hol et al.*, 2011]; (3) the molar volume of CO_2 at 40°C as a function of pressure (from equation of state by *Span and Wagner* [1996]). The coal is expected to adsorb slightly less CO_2 at 45°C than at 40°C, temperature at which swelling strains are measured. In the calculation performed here to estimate total adsorbed amounts from excess adsorbed amounts, we adopt the procedure proposed by *Ottiger et al.* [2006]. We thus neglect the effect of mesopores and adsorption-induced deformations on the adsorption process, which is a very simplistic approach. However, correctly interpreting gravimetric adsorption data by taking into account the full coupling between adsorption and strain still remains a challenging issue. While this issue is not fully solved, in addition to the interpretation proposed here, as alternatives, one can aim at using models based directly on excess adsorption data (e.g., *Vermorel et al.* [2013a, b]) or instead at measuring total adsorbed amounts directly (e.g., as proposed by *Hol et al.* [2011]).

In order to bound the inverted parameters, we follow two paths for the inversion procedure. First, we explore the anisotropy of adsorption-induced strains, and conclude that assuming isotropic and pressure-independent adsorption stresses is reasonable for the analyzed coal and permits recovering a plausible estimate of the coal mechanical anisotropy. Second, mechanical isotropy is assumed and the adsorption-strain coupling coefficients are recovered (still considered pressure-independent), so that, the anisotropy

of adsorption-strain coupling coefficients is determined. Last, we show that introducing a pressure-dependent coupling coefficients $c_1(p) \neq c_3(p)$ (based on the experimentally measured swelling strains and anisotropic mechanical elastic constants) enables a better the fitting of the experimental data.

3.1. Mechanical anisotropy and isotropic adsorption stresses

We first investigate whether adsorption-induced stresses can be assumed isotropic or not. According to our poromechanical model (Eq. 15), having equal coupling coefficients $c_1(p) = c_3(p)$ or equivalently $s_1^a(p) = s_3^a(p) = s^a(p)$ leads to,

$$\begin{cases} \varepsilon_1 &= [s^a(p) - p]\left(\frac{1-\nu}{E} - \frac{\nu_3}{E_3}\right) \\ \varepsilon_3 &= [s^a(p) - p]\left(\frac{1-2\nu_3}{E_3}\right) \end{cases} \tag{16}$$

which means that under such an assumption the ratio $\varepsilon_1/\varepsilon_3 = f(E, E_3, \nu, \nu_3)$ should be constant and independent of gas pressure and adsorption stresses. Figures 1-b and 1-e show the experimental ratios between the principal strains for both specimens. It is observed that $\varepsilon_1/\varepsilon_3$ and $\varepsilon_2/\varepsilon_3$ decrease slightly with pressure by about $\sim$10% for fluid pressure $p < 10$ MPa, which indicates slight anisotropy of adsorption stresses only in this range of pressure. Hence, as a first approximation we set adsorption stresses equal in all directions $s_1^a = s_3^a = s^a$ with constant adsorption coupling functions so that $c_1(p) = c_3(p) = c$. Assuming isotropic adsorption stresses leads to recovering an upper bound for mechanical anisotropy, which can be assessed by the parameter $(C_{11} - C_{33})/(2C_{33})$. Additional assumptions help reduce the number of inverted parameters: non-diagonal stiffness coefficients are approximately equal $C_{12} \sim C_{13}$ (as observed in many shales with weak anisotropy from an extensive data compilation by *Wang* [2002]), and one of the

Poisson ratios is assumed $\nu_3 = 0.28$ according to typical coal Poisson ratios determined indirectly from elastic waves velocity [*Morcote et al.*, 2010].

By assuming $C_{12} \sim C_{13}$, the following moduli ratio holds,

$$\frac{E}{E_3} = \frac{\nu_3 + \nu_3\nu - \nu}{\nu_3^2} \tag{17}$$

hence, given ν_3, $\nu = f(E/E_3)$. Given the total adsorbed amount and swelling principal strains of coal immersed in CO_2 as a function of pressure (ε_1, ε_2, ε_3), and a coupling coefficient c, the parameters n_0^{max} and β can be determined to best fit Eq. (9). Therefore, the free fitting parameters are E, E_3, and c. The shear modulus in planes which contain the symmetry axis G_3 is not needed for this particular application.

We fit our model simultaneously to the swelling strain and total adsorption amount data by forward simulation and 2-norm error estimation. Modeled strains ε_1 and ε_3 are set to fit experimentally measured $(\varepsilon_1 + \varepsilon_2)/2$ and ε_3 respectively. The calculated error surfaces are available as Auxiliary Material. Figures 1-a,c,d,f show the best-fitting modeling results along with the experimental data and best fitting parameters. Notice that E and E_3 are the specimen "dry" or "drained" moduli. The unjacketed response of the same specimens to Helium (specimen 364-1: $d\varepsilon_3/dp = 0.0050$ %/MPa, $d\varepsilon_1/dp \sim 0.0040$ %/MPa; specimen 364-2: $d\varepsilon_3/dp = 0.0049$ %/MPa, $d\varepsilon_1/dp \sim 0.0040$ %/MPa - original data set from *Hol and Spiers* [2012]) suggests stiffer moduli in the direction parallel to the bedding plane. From our inversion results, we indeed find that $E > E_3$. The inverted mechanical anisotropy in terms of the Thomsen parameter $\varepsilon^* = (C_{11} - C_{33}/(2C_{33})$ is about 0.137 (specimen 364-1) and 0.082 (specimen 364-2), in agreement with Thomsen parameters measured in other coals $\varepsilon^* \sim 0.05 - 0.10$ [*Morcote et al.*, 2010] and shales $\varepsilon^* = 0.17 \pm 0.08$ [*Wang*, 2002].

Inverted bulk moduli K=4.21 GPa for specimen 364-1 and K=3.58 GPa for specimen 364-2 are in the range of values for bituminous coal: 0.79 to 5.3 GPa (spanning several scales and loading rates [*Mazumder*, 2007; *Morcote et al.*, 2010; *Pan et al.*, 2010; *Masoudian et al.*, 2013]).

3.2. Mechanical isotropy and anisotropic adsorption stresses

Let us now assume isotropic mechanical properties and find the pressure-independent adsorption-strain coupling coefficients c_1 and c_3 which best fit the experimental data. Having $E = E_3$ and $\nu = \nu_3$, Eq. (15) leads to

$$\begin{cases} \varepsilon_1 &= \frac{1-\nu}{E}\left[s_1^a(p) - p\right] - \frac{\nu}{E}\left[s_3^a(p) - p\right] \\ \varepsilon_3 &= -\frac{2\nu}{E}\left[s_1^a(p) - p\right] + \frac{1}{E}\left[s_3^a(p) - p\right] \end{cases} \tag{18}$$

We simplify the problem similarly as done above by assuming one known Poisson ratio $\nu = 0.28$. Foward simulation and error estimation let us recover the best fitting parameters E, c_1, and c_3. Figure 2 shows the simulation results for the best fitting parameters. Auxiliary Material contains the error surfaces for best fitting parameter determination. The fact that $c_3 > c_1$ implies that adsorption stresses would be higher in the direction perpendicular to the bedding plane. We find that the upper bound for adsorption stress anisotropy is $(c_3 - c_1)/(2c_1) \sim 0.048$ for specimen 364-1 and 0.030 for specimen 364-2. The fitting is overall poorer than the one observed by concentrating anisotropy on mechanical elastic moduli.

3.3. Pressure-dependent adsorption-strain coupling coefficients

Let us use now the values of E_3, E, ν_3, and ν found in Section 3.1 and relax the previous assumption of pressure-independent coupling coefficients. By taking the derivatives of Eq.

(15) with respect to pressure and multiplying by the inverse of the compliance matrix, the following holds,

$$\begin{bmatrix} \frac{ds_1^a(p)}{dp} - 1 \\ \frac{ds_3^a(p)}{dp} - 1 \end{bmatrix} = \begin{bmatrix} \frac{1-\nu}{E} & -\frac{\nu_3}{E_3} \\ -2\frac{\nu_3}{E_3} & \frac{1}{E_3} \end{bmatrix}^{-1} \begin{bmatrix} \frac{d\varepsilon_1}{dp} \\ \frac{d\varepsilon_3}{dp} \end{bmatrix} \tag{19}$$

Hence, calculating the value of $ds_i^a(p)/dp$, the coupling coefficients follow from Eq. (12) and are equal to $c_i(p) \sim 8$ to 11 (Figure 3-a,c - Note: $d\varepsilon_1/dp$ is calculated from experimental $(\varepsilon_1 + \varepsilon_2)/2$ as a function of pressure). The difference between $c_3(p)$ and $c_1(p)$ is maximum at pressure $p < 10$ MPa as sugested by Figure 1. The lower bound for anisotropy of adsorption stresses is estimated with the average difference $\overline{|c_3 - c_1|}/(2\overline{c_1})$ equal to 0.013 for specimen 364-1 and 0.011 for specimen 364-2. We find that assuming a constant coupling coefficient with pressure does not capture perfectly the coal matrix linear compressibility observed experimentally at high pressures $p > 10$ MPa (See Figures 1-a-d). In contrast, a better curve matching is observed by considering pressure-dependent coupling coefficients $c_1(p) \neq c_3(p)$. The recalculated swelling strains are plotted with the refitted adsorption variables n_0^{max} and β in Figure 3-b,d for both specimens.

4. Discussion

4.1. Comparison with empirical approaches and and non-empirical theories

Early empirical developments simplify the effect of coal swelling in reservoir geomechanics to be analogous to that of thermal dilation [*Palmer and Mansoori*, 1998; *Shi and Durucan*, 2004], such that, coal swelling is expressed empirically by fitting a Langmuir isotherm directly to swelling strains, or assuming a linear relationship between swelling and Langmuir-fitted adsorption amount (See a comprehensive review in *Pan and Connell*

[2012]). Such empirical developments are sometimes too simplistic, as here for instance, monotonic Langmuir functions would not be able to fit well the non-monotonic swelling strains shown in Figure 1.

Other non-empirical models have been recently proposed to explain and predict the adsorption-induced swelling of coal. First, *Hol and Spiers* [2012] proposed a thermodynamical model to explain the Brzeszcze coal swelling data we use in this article. They base their formulation on the separation of adsorption-induced swelling and bulk fluid-driven compression (similar to Eq. 15), with the additional hypothesis of a linear relationship between total adsorption amount and adsorption strain. Our model shows fair agreement with this hypothesis for samples immersed in the adsorbate at low gas pressure $p < 10$ MPa, although deviations may occur at higher pressures when the bulk fluid pressure compression of the coal matrix prevails decreasing the total amount of adsorption (Figure 1-c,f). Anisotropy modeling is not included by *Hol and Spiers* [2012], although it has been considered by the same authors elsewhere [*Hol et al.*, 2012]. Second, *Vermorel et al.* [2013a] developed a poromechanical formulation based on properties defined at the molecular scale, such as microporosity or microporous skeleton stiffness K_s. This formulation proposes an adsorption-mechanical coupling based on the definition of an apparent microporosity which depends on excess n_{ex} and total n_t adsorbed amounts. We find the isotropic version of our formulation compatible with theirs if $\partial n/\partial \epsilon|_p = (1 - K/K_s)n_t/(n_t - n_{ex})$ where ϵ is the volumetric deformation (see Eq. 11). Third, *Pan and Connell* [2011] developed a swelling model for mesoporous solids which includes orthotropy. They base their model on a crossed-tube analogous structure. In contrast, our model does not assume a particular geometry and mechanical properties ensues naturally from continuum

mechanics. Last, *Coudert et al.* [2011] present a general thermodynamical formulation of adsorption-strain couplings in soft microporous zeolites and metal organic frameworks. Their formulation shares many common points with our model.

All these non-empirical models have shown an advance in adsorption-strain understanding and good fitting results. We believe our model is thermodynamically and mechanically rigorous, based on well-defined quantities, valid for any strain or stress boundary conditions, and easily expandable to more complex constitutive laws (orthotropy, non-linearity). Our theoretical model has the key advantage over empirical developments of having fully coupled equations which relate adsorption not only to strain but also to stress. Furthermore, our model enables the prediction of the influence of adsorption on strains and stresses as well as the influence of stresses and strains on the amount of adsorbed fluid. The prediction of stresses is advantageous to use permeability-stress laws instead of permeability-porosity laws.

4.2. Adsorption isotherms for samples immersed in the adsorbate

We emphasize that adsorption isotherms of free-swelling coal samples immersed in the adsorbate represent just one path on the multivariate adsorption isotherm $n(p, \varepsilon_{ij})$ which describes how total adsorbed amount depends on fluid pressure and solid strains. Thus, the measurements from this kind of experiments are only relevant to this pressure-strain path and are not representative of the adsorption isotherm with the real boundary in-situ conditions. As shown in Figures 1-c,f and 2-b,d, the difference in adsorbed amount for a coal sample immersed in CO_2 (displacement-unconstrained, free swelling) and coal sample kept at zero strain is $\sim 20\%$. External confining stresses, estimated at about about ~ 90 MPa with our model, must be applied in order to prevent any deformation of the

Brzeszcze coal sample (CO_2 pressure $p = 10$ MPa - from $\varepsilon_{ij} = 0$ in Eq. 13). In-situ conditions lie in between these two scenarios. In general, the adsorption isotherm is a multivariate function which depends on pressure and strains. Hence, there may be adsorption/desorption at constant fluid pressure driven by strain changes such as mechanical stretching and compression (Eq. 11 - See experimental evidence in [*Hol et al.*, 2012; *Hol and Spiers*, 2012]).

4.3. Relation between volumetric strain and total adsorption for samples immersed in the adsorbate

Our model predicts an approximately linear relationship between total adsorption amount and strain when adsorption-induced swelling prevails for adsorption experiments with coal samples immersed in the adsorbate, i.e., at low-medium fluid pressure (Figure 4-a,b, $p < 10$ MPa). However, as predicted by our model (no adsorption amount experimental data in this pressure range), total adsorption amount may decrease as bulk fluid pressure takes more relevance and compresses the coal matrix. Improved certainty in the determination of total adsorption amount n would help corroborate this last statement. Recall the fact that we follow a Lagrangian mechanical description, therefore, adsorption per unit volume of undeformed coal matrix [mol/L] may be converted to adsorption per unit mass [mol/kg] through the initial mass density [kg/L]. Recently published experimental data of simultaneous measurement of adsorption and swelling up to 15 MPa show a similar shape of the swelling-adsorption signature as the one predicted by our model before the onset of coal matrix contraction (see Fig. 8 from *Day et al.* [2008]). Other phenomena that may affect the shape of the adsorption-strain curve include creep at con-

stant Terzaghi's effective stress and coal matrix adsorption-induced softening [*Czaplinski and Holda*, 1982; *Hagin and Zoback*, 2010; *Masoudian et al.*, 2013].

4.4. Adsorption-strain coupling expressed with Biot-like coefficients

The Biot coefficient α was first defined as the ratio of change in fluid content ζ to dilation ϵ in a jacketed (drained) test, such that for a conventional poroelastic material $\zeta = \alpha\epsilon$ [*Biot and Willis*, 1957]. Biot noted that α can also be identified to $1 - K/K_{sk}$ (where K and K_{sk} are the bulk moduli measured in drained and unjacketed conditions) which provides a further interpretation of α different from the first definition. The fact that they yield equal values results from the symmetry of the coefficients in the poroelastic matrix and in turn from the existence of a thermodynamic potential with pressure p and change in fluid content ζ as conjugate variables. In conventional poroelasticity the density of the fluid into the porosity of the material corresponds to its bulk density, therefore, the Biot coefficient α is less than 1 as the volume of fluid ζ entering the specimen during a drained test cannot be greater than its dilation ϵ.

However, this is not the case in adsorptive materials such as coal where the density of the adsorbed fluid can be much greater than the density of the bulk fluid. In the framework of the theory developed here for transverse isotropic microporous solids, the incremental amount of fluid content $d\zeta = d(n\overline{V}_b)$ during a jacketed test is (from Eq. 9)

$$d[n(p, \varepsilon_{ij})\overline{V}_b(p)] = b_1(p)d\varepsilon_1 + b_1(p)d\varepsilon_2 + b_3(p)d\varepsilon_3 \tag{20}$$

where $b_i(p) = c_i(p)n_0(p)\overline{V}_b(p)$ can be coined as a (tangent) Biot-like coefficient, consistently with the first definition given by Biot. The fluid content $n\overline{V}_b$ is the volume (per

unit volume of coal) that the amount of adsorbed fluid would occupy in it were in bulk conditions. Therefore the volume change $d(n\overline{V}_b)$ can be much larger than the volumetric dilation increment $d\epsilon$ leading to coefficients $b_i(p)$ exceeding 1. This does not contradict thermodynamics. Due to the symmetry already discussed, this coefficient $b_i(p)$ can still be identified to $1 - K/K_{unj}$ which is equal to ds_i^a/dp here (Eq. 12), but the unjacketed bulk modulus $K_{unj}(p)$ does not reveal the solid stiffness alone. It is a macroscopic property which also accounts for the adsorptive properties of the fluid molecules onto the solid pore walls. *Vermorel et al.* [2013b] defines an analogous Biot-like pressure-dependent coefficient as $b(p) = b^\infty n_T(p)/[n_T(p) - n_{excess}(p)]$ where $b^\infty < 1$ is the asymptotic Biot coefficient obtained at high fluid pressure.

Given the coal adsorption properties (n_0^{max}, β, c_i) and the CO_2 bulk molar volume $\overline{V}_b$, the Biot-like coefficient ranges from $b^t \sim 40$ to 1 for low CO_2 pressure $p = 0$ to ~ 10 MPa (adsorption prevails) and decreases asymptotically to ~ 0.74 as CO_2 pressure increases (plotted in Figure 4-c,d as solid line for pressure-independent c and as symbols for pressure-dependent $c_i(p)$). The $b(p)$ curve exhibits an inflexion point which roughly coincides with the limit between adsorption-dominated swelling $b > 1$ and bulk fluid-driven compression $b < 1$ (Figure 4-c,d).

Although they remain nontrivial, variations of the introduced Biot-like coefficients b_i with the fluid pressure are simpler than variations of the coupling coefficients c_i, in the sense that at least the former are monotonic. The complexity of the variations of the coefficients $c_i(p)$ stems from the fact that those coefficients involve characteristics of the solid, of the fluid, and of their interaction. In contrast, since $b_i(p) = c_i(p)n_0(p)\overline{V}_b(p)$, the Biot-like coefficients are corrected for variations of density of the bulk fluid. Therefore,

when looking for a physical interpretation of the inverted parameters of the model, one might find more useful focusing on the Biot-like coefficients rather than on the more convoluted coupling coefficients c_i. For instance, in the isotropic case, *Vermorel et al.* [2013b] propose the physical rule of thumb that the Biot-like coefficient $b(p)$ is proportional to the ratio of the density ρ_{sorbed} of the adsorbed phase to the density ρ_{free} of the bulk phase (i.e., $b(p) \propto \rho_{sorbed}(p)/\rho_{free}(p)$.

4.5. Implications for coal bed methane recovery

The determination of strains and effective stress on the direction of the bedding plane in coal seams subjected to primary or secondary methane recovery is critical to predict changes in fracture permeability. Various permeability-stress relationships have been proposed to predict permeability, generally in the form: $\log(k/k_0) = a(\sigma_h + p - \sigma_{h0} - p_0)$ (being k_0 the reference permeability at total horizontal stress σ_{h0} and fluid pressure p_0 and $a \sim 0.1$ to 0.2 MPa^{-1}[*Somerton et al.*, 1975; *Pan and Connell*, 2012]). Thus, a general model that predicts stresses in the anisotropic coal seam as a function of fluid pressure and boundary conditions is required for realistic predictions and simulations of coal bed methane recovery. The coal seam can be modeled as a double-porosity reservoir rock, where cleats account for macroporosity and coal matrix micropores account for the microporosity. In order to become practical at the scale of the seam, the constitutive laws derived here at the scale of the coal matrix must be upscaled to the scale of the coal seam by incorporating the presence of the cleats, in the spirit of what was done by *Nikoosokhan et al.* [2012]. In this upscaling, the presence of the cleats only induces regular poromechanical effects, in the sense that cleats are macropores in which adsorption-effects are negligible, and the coal matrix is responsible for adsorption-induced phenomena. This

extension of our model will allow to incorporate, in a thermodynamically sound manner, both anisotropy and adsorption-induced phenomena into the constitutive laws of coal seams.

5. Conclusions

Coal matrix is a natural disordered microporous solid. Material properties are often anisotropic due to sedimentation and diagenetic processes. Although coal adsorptive properties have been widely studied, the physical link between adsorption and induced-strain has been relegated to a second plane. The knowledge of adsorptive and mechanical properties is critical for calculating coal bed gas reserves and storage capacity, and enabling predictable exploitability.

We extended a poromechanical model developed for microporous solids to take into account adsorptive-mechanical anisotropy through adsorption stresses and a stiffness matrix. Our model ensues from first principles and continuum mechanics, and applies to any displacement or stress boundary conditions.

Experimental data from the literature help validate our model and invert adsorptive-mechanical model parameters. The model is able to simulate the competition between adsorption-induced adsorption and bulk fluid-driven compression in adsorption experiments of coal samples immersed in CO_2.

Remarkable lessons from this study and the Brzeszcze coal include: (1) swelling anisotropy is likely to be caused principally by mechanical anisotropy ($E > E_3$), in fact, concentrating anisotropy on elastic moduli yields better fitting than concentrating anisotropy on adsorption stresses, (2) assuming a coupling coefficient c independent of fluid pressure is reasonable and yields acceptable predictions, (3) adsorption measurements

in coal samples immersed in the adsorbate represent just one path on the multivariate adsorption isotherm.

The developed fully coupled model permits inverting transverse isotropic mechanical-adsorptive properties of microporous coal matrix. Upscaling to a coal seam model which includes both macroporous cleats and microporous adsorptive coal matrix would yield the coupled constitutive equations of the coal seam. This set of fully coupled equations enable the prediction of strains and effective stress in different directions respect to the bedding plane under in-situ anisotropic state of stresses. The calculated effective stresses can be used through permeability-stress relationships for determining seam permeability.

Acknowledgments. This work was supported by Total S.A. We are thankful to R. Vermorel, the associate editor, and anonymous reviewers for insightful comments.

References

Biot, M. A. and D. G. Willis (1957), The elastic coefficients of the theory of consolidation, *Journal of Applied Mechanics*, *24*, 594–601.

Brochard, L., M. Vandamme, and R.-M. Pellenq (2012), Poromechanics of microporous media, *Journal of the Mechanics and Physics of Solids*, *60*(4), 606–622, doi:10.1016/j.jmps.2012.01.001.

Busch, A., S. Alles, Y. Gensterblum, D. Prinz, D. Dewhurst, M. Raven, H. Stanjek, and B. Krooss (2008), Carbon dioxide storage potential of shales, *International Journal of Greenhouse Gas Control*, *2*(3), 297–308, doi:10.1016/j.ijggc.2008.03.003.

Ceglarska-Stefanska, G., and A. Czaplinski (1993), Correlation between sorption and dilatometric processes in hard coals, *Fuel*, *72*, 413–417.

Ceglarska-Stefanska, G., and K. Zarebska (2002), The competitive sorption of CO2 and CH4 with regard to the release of methane from coal, *Fuel Processing Technology*, *77-78*, 423–429.

Cheng, A. H. -D. (1997), Material coefficients of anisotropic poroelasticity, *International Journal of Rock Mechanics and Mining Sciences*, *34*(2), 199–205.

Cody, G. D., J. W. Larsen, and M. Siskin (1988), Anisotropic solvent swelling of coals, *Energy & Fuels*, *2*(3), 340–344, doi:10.1021/ef00009a020.

Coudert, F.-X., A. Boutin, M. Jeffroy, C. Mellot-Draznieks, and A. H. Fuchs (2011), Thermodynamic methods and models to study flexible metal-organic frameworks., *Chemphyschem : a European journal of chemical physics and physical chemistry*, *12*(2), 247–58, doi:10.1002/cphc.201000590.

Coussy, O. (2004), *Poromechanics*, 298p., Wiley.

Coussy, O. (2010), *Mechanics and Physics of Porous Solids*, 281p., Wiley.

Cowin, S. C. (2004), Anisotropic poroelasticity: fabric tensor formulation, *Mechanics of Materials*, *36*, 665–677.

Cui, X., R. M. Bustin, and L. Chikatamarla (2007), Adsorption-induced coal swelling and stress: Implications for methane production and acid gas sequestration into coal seams, *Journal of Geophysical Research*, *112*(B10202), doi:10.1029/2004JB003482.

Czaplinski, A., and S. Holda (1982), Changes in mechanical properties of coal due to sorption of carbon dioxide vapour, *Fuel*, *61*, 1281–1282.

Day, S., R. Fry, and R. Sakurovs (2008), Swelling of Australian coals in supercritical CO2, *International Journal of Coal Geology*, *74*(1), 41–52, doi:10.1016/j.coal.2007.09.006.

Day, S., R. Fry, R. Sakurovs, and S. Weir (2010), Swelling of Coals by Supercritical Gases and Its Relationship to Sorption, *Energy & Fuels*, *24*(4), 2777–2783, doi: 10.1021/ef901588h.

Ding, H., W. Chen, and L. Zhang (2006), *Elasticity of transversely isotropic materials*, 444 pp., Springer.

Fowler, R. H. (1935), A statistical derivation of Langmuirs adsorption isotherm, *Mathematical Proceedings of the Cambridge Philosophical Society*, *31*(2), 260–264.

Gensterblum, Y., P. V. Hemert, P. Billemont, E. Battistutta, A. Busch, B. Krooss, G. D. Weireld, and K. Wolf (2010), European inter-laboratory comparison of high pressure CO2 sorption isotherms II: Natural coals, *International Journal of Coal Geology*, *84*(2), 115–124, doi:10.1016/j.coal.2010.08.013.

Hagin, P., and M. D. Zoback (2010), Laboratory studies of the compressibility and permeability of low-rank coal samples from the Powder River Basin, Wyoming, USA, in *ARMA 10-170*.

Hol, S., C. J. Peach, and C. J. Spiers (2011), A new experimental method to determine the CO2 sorption capacity of coal, *Energy Procedia*, *4*, 3125–3130.

Hol, S., C. J. Peach, and C. J. Spiers (2011), Applied stress reduces the CO2 sorption capacity of coal, *International Journal of Coal Geology*, *85*(1), 128–142, doi: 10.1016/j.coal.2010.10.010.

Hol, S., and C. J. Spiers (2012), Competition between adsorption-induced swelling and elastic compression of coal at CO2 pressures up to 100MPa, *Journal of the Mechanics and Physics of Solids*, *60*(11), 1862–1882, doi:10.1016/j.jmps.2012.06.012.

Hol, S., C. J. Peach, and C. J. Spiers (2012), Effect of 3-D stress state on adsorption of CO2 by coal, *International Journal of Coal Geology*, *93*, 1–15, doi:10.1016/j.coal.2012.01.001.

Johnston, J. E., and N. I. Christensen (1995), Seismic anisotropy of shales, *Journal of Geophysical Research*, *100*(B4), 5991–6003.

Kowalczyk, P., A. Ciach, and A. V. Neimark (2008), Adsorption-induced deformation of microporous carbons: pore size distribution effect., *Langmuir : the ACS journal of surfaces and colloids*, *24*(13), 6603–8, doi:10.1021/la800406c.

Levine, J. R. (1996), Model study of the influence of matrix shrinkage on absolute permeability of coal bed reservoirs, *Geological Society, London, Special Publications*, *109*, 197–212, doi:10.1144/gsl.sp.1996.109.01.14.

Masoudian, M., D. Airey, and A. El-Zein (2013), A chemo-poro-mechanical model for sequestration of carbon dioxide in coalbeds, *Geotechnique*, *63*(3), 235–243.

Mazumder, S. (2007), Dynamics of CO2 in coal as a reservoir, Ph.D. thesis, Delft University.

Mazumder, S., A. Karnik, and K. H. Wolf (2006), Swelling of coal in response to CO2 sequestration for ECBM and its effect on fracture permeability, *SPE Journal*,*11*(3), pp. 390–398.

Moffat, D. H., and K. E. Weale (1954), Sorption by coal of methane at high pressure, *Fuel*, *34*, 449–462.

Morcote, A., G. Mavko, and M. Prasad (2010), Dynamic elastic properties of coal, *Geophysics*, *75*(6), E227, doi:10.1190/1.3508874.

Neimark, A. V., F.-X. Coudert, C. Triguero, A. Boutin, A. H. Fuchs, I. Beurroies, and R. Denoyel (2011), Structural transitions in MIL-53 (Cr): view from outside and

534 inside., *Langmuir : the ACS journal of surfaces and colloids*, *27*(8), 4734–41, doi:
535 10.1021/la200094x.

536 Nikoosokhan, S., M. Vandamme, P. Dangla (2012), A poromechanical model for coal
537 seams injected with carbon dioxide: from an isotherm of adsorption to a swelling of
538 the reservoir, *Oil & Gas Science and Technology Rev. IFP, Energies nouvelles*, *67*(5),
539 777–786.

540 Ottiger S., R. Pini, G. Storti, M. Mazzotti, R. Bencini, F. Quattrocchi, G. Sardu, and
541 G. Deriue (2006), Adsorption of pure carbon dioxide and methane on dry coal from
542 the Sulcis coal province (SW Sardinia, Italy), *Environmental Progress*, *25*(4), 355–364,
543 doi:10.1002/ep.10169.

544 Palmer, I., and J. Mansoori (1998), How Permeability Depends on Stress and Pore Pres-
545 sure in Coalbeds: A New Model, *Evaluation*, (December), 539–544.

546 Pan, Z., and L. D. Connell (2011), Modelling of anisotropic coal swelling and its impact
547 on permeability behaviour for primary and enhanced coalbed methane recovery, *Inter-*
548 *national Journal of Coal Geology*, *85*(3-4), 257–267, doi:10.1016/j.coal.2010.12.003.

549 Pan, Z., L. D. Connell, and M. Camilleri (2010), Laboratory characterisation of coal
550 reservoir permeability for primary and enhanced coalbed methane recovery, *Interna-*
551 *tional Journal of Coal Geology*, *82*, 252–261.

552 Pan, Z. J., and L. D. Connell (2007), A theoretical model for gas adsorption-induced coal
553 swelling, *International Journal of Coal Geology*, *69*, 243–252.

554 Pan, Z. J., and L. D. Connell (2012), Modelling permeability for coal reservoirs: A review
555 of analytical models and testing data, *International Journal of Coal Geology*, *92*, 1–44.

Pekot, J. L., and S. R. Reeves (2002), Modeling coal matrix shrinkage and differential swelling with CO2 injection for enhanced coalbed methane recovery and carbon sequestration applications, *Tech. rep.*, Advanced Resources International, Houston, Texas.

Pijaudier-Cabot, G., R. Vermorel, C. Miqueu, and B. Mendiboure (2011), Revisiting poromechanics in the context of microporous materials, *Comptes Rendus Mécanique*, *339*(12), 770–778, doi:10.1016/j.crme.2011.09.003.

Pini, R., S. Ottiger, G. Storti, and M. Mazzotti (2009), Pure and competitive adsorption of CO2, CH4 and N2 on coal for ECBM, *Energy Procedia*, *1*(1), 1705–1710, doi:10.1016/j.egypro.2009.01.223.

Pone, J. D. N., P. M. Halleck, and J. P. Mathews (2009), Sorption Capacity and Sorption Kinetic Measurements of CO2 and CH4 in Confined and Unconfined Bituminous Coal, *Energy & Fuels*, *23*(9), 4688–4695, doi:10.1021/ef9003158.

Ravikovitch, P. I., and A. V. Neimark (2006), Density functional theory model of adsorption deformation., *Langmuir : the ACS journal of surfaces and colloids*, *22*(26), 10,864–8, doi:10.1021/la061092u.

Reucroft, P. J., and A. R. Sethuraman (1987), Effect of pressure on carbon dioxide induced coal swelling, *Energy Fuels*, *1*, 72–75.

Slatt, R. M., and Y. Abousleiman (2011), Merging sequence stratigraphy and geomechanics for unconventional gas shales, *The Leading Edge*, *30*(3), 274–282, doi:10.1190/1.3567258.

Shi, J. Q., and S. Durucan (2004), Drawdown induced changes in permeability of coalbeds: A new interpretation of the reservoir response to primary recovery, *Transport in Porous Media*, *56*, 1–16.

579 Sloan, E. D., and C. A. Koh (2008), *Clathrate hydrates of natural gases - Third edition*,
580 701 ST – Clathrate hydrates of natural gases – Th pp., CRC Press, Boca Raton, FL.
581 Somerton, W. H., I. M. Soylemezoglu, and R.C. Dudley (1975), Effect of stress on per-
582 meability of coal, *Int. J. Rock Mech. Min. Sci. & Geomech. Abstr.*, *12*, 129–145.
583 Span, R., and W. Wagner (1996), A new equation of state for carbon dioxide covering the
584 fluid region from the triple-point temperature to 1100 K at pressures up to 800 MPa,
585 *Journal of Physical and Chemical Reference Data*, *25*, 1509–1596.
586 Thomsen, L. (1986), Weak elastic anisotropy, *Geophysics*, *51*(10), 1954–1966.
587 Ulm, F.-J., M. Vandamme, C. Bobko, J.A. Ortega, K. Tai, and C. Ortiz (2007), Sta-
588 tistical Indentation Techniques for Hydrated Nanocomposites: Concrete, Bone, and
589 Shale, *Journal of the American Ceramic Society*, *90*(9), 2677–2692, doi:10.1111/j.1551-
590 2916.2007.02012.x.
591 van Bergen, F., S. Hol, and C. Spiers (2011), Stressstrain response of pre-compacted
592 granular coal samples exposed to CO2, CH4, He and Ar, *International Journal of Coal*
593 *Geology*, *86*(2-3), 241–253, doi:10.1016/j.coal.2011.02.007.
594 Vandamme M., L. Brochard, B. Lecampion, and O. Coussy (2010), Adsorption and strain:
595 The CO2-induced swelling of coal, *Journal of Mechanics and Physics of Solids*, *58*,
596 1489–1505.
597 Vandenbroucke, M., and C. Largeau (2007), Kerogen origin, evolution and structure,
598 *Organic Geochemistry*, *38*(5), 719–833, doi:10.1016/j.orggeochem.2007.01.001.
599 Vermorel, R., G. Pijaudier-Cabot, C. Miqueu, and B. Mendiboure (2013), 2. Poromechan-
600 ics of Saturated Isotropic Nanoporous Materials, in *Damage Mechanics of Cementitious*
601 *Materials and Structures, eds.: G. Pijaudier-Cabot and F. Dufour.*

Vermorel, R., and G. Pijaudier-Cabot (2013b), Enhanced continuum poromechanics to account for adsorption induced swelling of saturated isotropic nanoporous materials, in *Poromechanics V, eds.: C. Hellmich, B. Pichler, and D. Adam.*

Vernik, L., and A. Nur (1992), Ultrasonic velocity and anisotropy of hydrocarbon source rocks, *Geophysics*, *57*(5), 727–735.

Wang, Z. (2002), Seismic anisotropy in sedimentary rocks, part 2: Laboratory data, *Geophysics*, *67*(5), 1423–1440.

Wang S., D. Elsworth, and J. Liu (2011), Permeability evolution in fractured coal: The roles of fracture geometry and water-content, *International Journal of Coal Geology*, *87*(1), 13–25, doi:10.1016/j.coal.2011.04.009.

Weniger, P., W. Kalkreuth, A. Busch, and B. M. Krooss (2010), High-pressure methane and carbon dioxide sorption on coal and shale samples from the Paraná Basin, Brazil, *International Journal of Coal Geology*, *84*(3-4), 190–205, doi:10.1016/j.coal.2010.08.003.

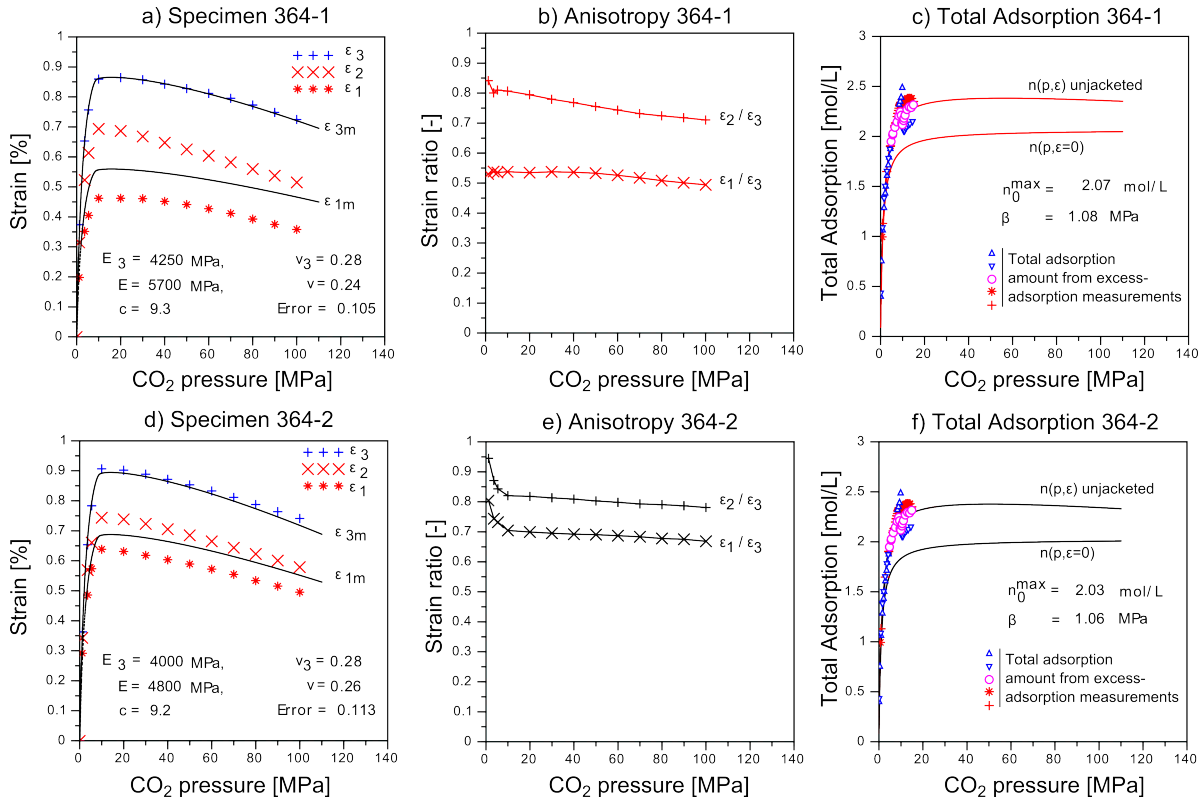

Figure 1. Adsorption-induced swelling of coal immersed in CO_2. (a) Experimental measurements (symbols: principal strains $\varepsilon_1, \varepsilon_2, \varepsilon_3$ - original data set from *Hol and Spiers* [2012]) and transverse isotropic microporous model predictions considering mechanical anisotropy only $c_1(p) = c_3(p) = c$ (lines: $\varepsilon_{1m}, \varepsilon_{3m}$ fit $(\varepsilon_1 + \varepsilon_2)/2$ and ε_3 respectively). (b) Swelling anisotropy: strain ratios ε_1 and ε_2 respect to the major principal strain ε_3 perpendicular to the bedding plane. (c) Total adsorption amount estimated from excess sorption measurements (symbols - see Auxiliary Material) and model fitted prediction (Eq. 9). (a,b,c) Specimen 364-1. (d,e,f) Specimen 364-2.

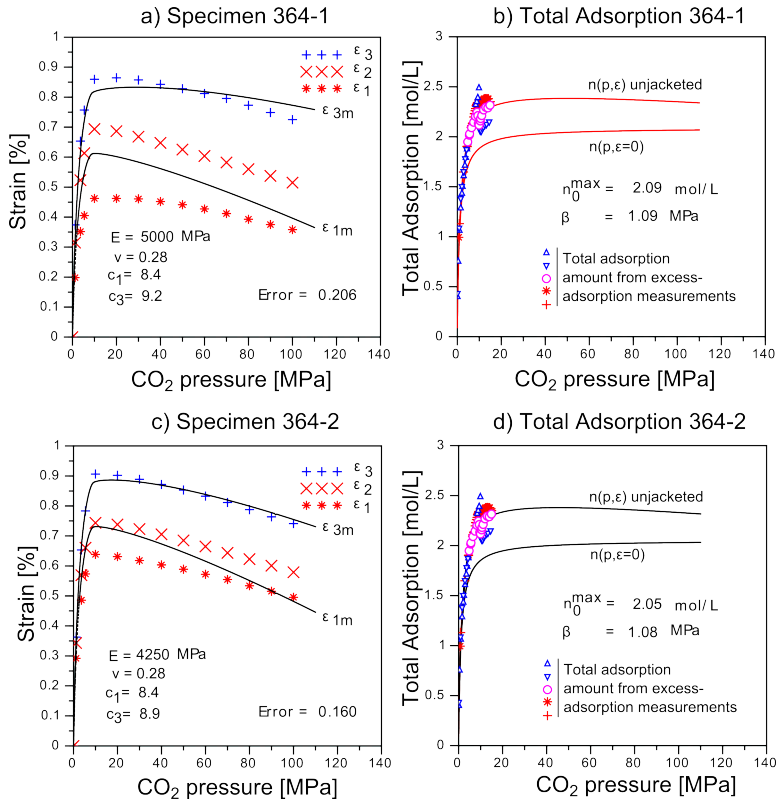

Figure 2. Adsorption-induced swelling of coal immersed in CO_2. (a) Experimental measurements (symbols: principal strains $\varepsilon_1, \varepsilon_2, \varepsilon_3$ - original data set from *Hol and Spiers* [2012]) and transverse isotropic microporous model predictions considering anisotropy on adsorption stresses only $E = E_3$ and $\nu = \nu_3$ (lines: $\varepsilon_{1m}, \varepsilon_{3m}$ fit $(\varepsilon_1 + \varepsilon_2)/2$ and ε_3 respectively). (b) Total adsorption amount estimated from excess sorption measurements (symbols - Auxiliary Material) and model fitted prediction (Eq. 9). (a,b) Specimen 364-1. (c,d) Specimen 364-2.

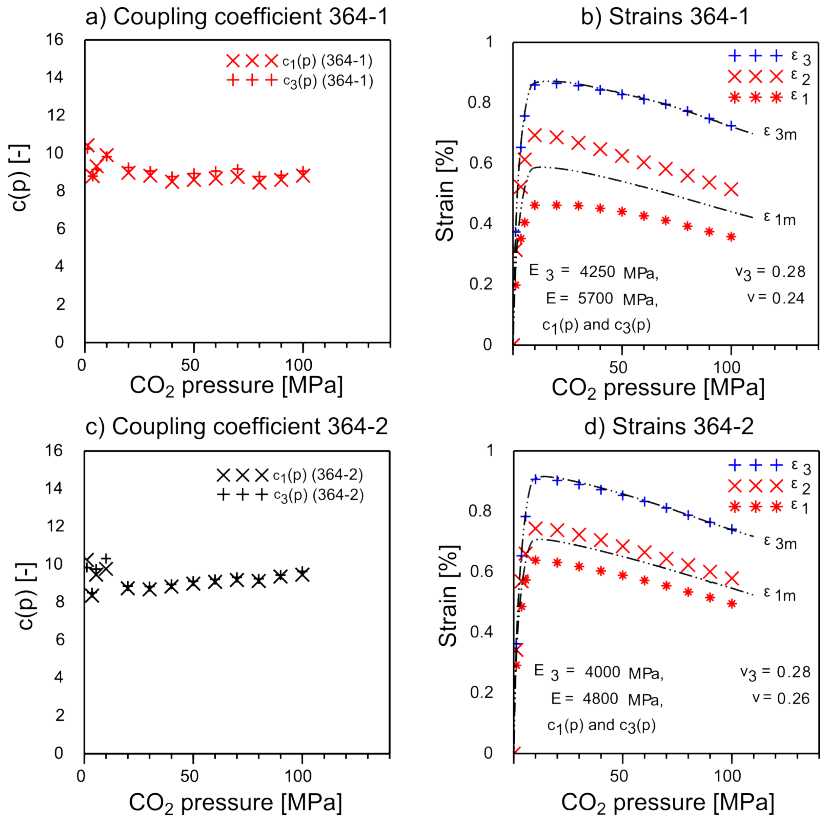

Figure 3. Determination of adsorption-strain coupling coefficients as a function of pressure for finding minimum adsorption stress anisotropy. (a) Calculated coupling coefficient $c_i(p)$ in the bedding plane and perpendicular to the bedding plane (Eq. 19). (b) Transverse isotropic microporous model predictions (lines: $\varepsilon_{1m}, \varepsilon_{3m}$) considering $c_i(p)$ previously calculated and refitted n_0^{max} and β compared to experimental data - original data set from *Hol and Spiers* [2012]. (a,b) Specimen 364-1 - refitted $n_0^{max} = 2.04$ mol/L and $\beta = 1.08$. (d,e) Specimen 364-2 - refitted $n_0^{max} = 2.00$ mol/L and $\beta = 1.06$.

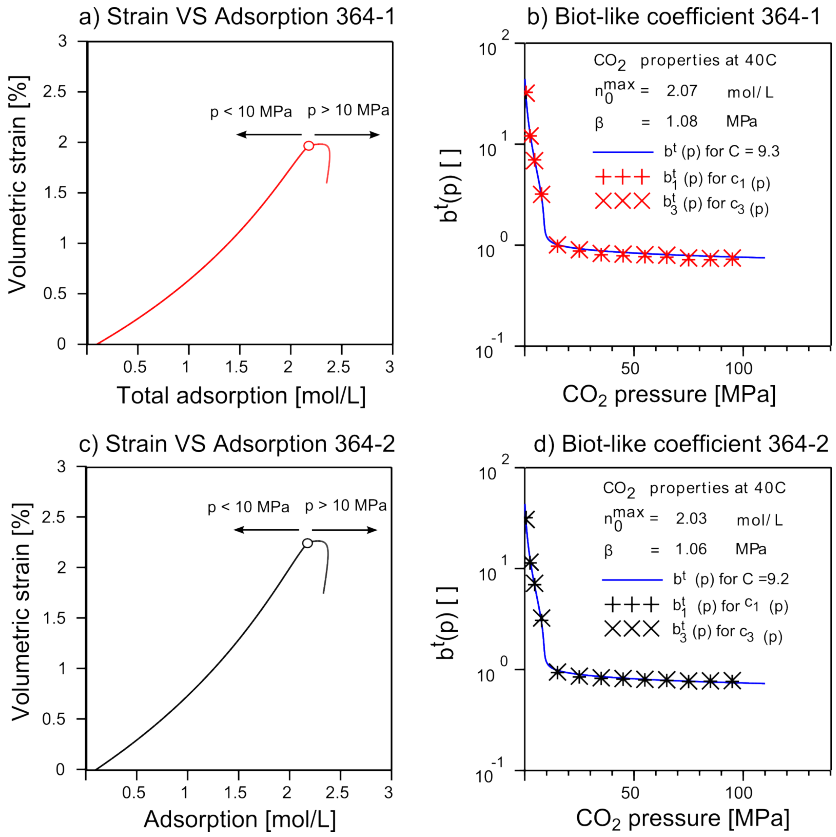

Figure 4. Insight into the poromechanics of coal matrix. (a) Model-predicted volumetric strain as a function of total adsorption amount for coal immersed in CO_2 (model parameters from Figure 1). (b) Biot-like pressure dependent functions $b_i^t(p)$. (a,b) Specimen 364-1. (c,d) Specimen 364-2.